Analytical Modeling of No-Vent Fill Process

David A. Vaughan*
Martin Marietta Manned Space Systems, Huntsville, Alabama 35812
and
George R. Schmidt†
NASA Marshall Space Flight Center, Huntsville, Alabama 35812

This paper describes a finite difference computer model that predicts no-vent fill performance in a 1-g environment. Derived from the Shuttle External Tank pressurization code, the model accounts for several major effects that influence the process, such as tank and fluid inlet temperature, interfacial mass transfer, and inlet jet characteristics. The paper also explains how ground test data with Freon-114 were used to validate the model's accuracy and to compare, over a restricted range of inflow regimes ($0.1 < z/D < 2.0$), experimentally measured condensation rates with predictions from universal submerged jet theory.

Nomenclature

A = area
C = specific heat (incompressible material)
C_p = isobaric specific heat
C_v = isochoric specific heat
D = characteristic diameter
d = nozzle diameter
Gr = Grashoff Number
H = enthalpy
H_{fg} = latent heat of vaporization
h = heat transfer coefficient
k = thermal conductivity
L = characteristic length
M = mass
m = mass flow rate
P = pressure
Pr = Prandtl number
Q = heat flow rate
q = heat flux
St = Stanton number
T = temperature
t = time
U = internal energy
V = volume
w = rate of work
z = liquid height

Subscripts

a = ambient
b = boiloff
con = condensate
cond = conduction
f = interface
g = ullage gas
in = inlet
l = liquid
n = insulation
s = surface
sat = saturation
t = tank
w = tank wall

Presented as Paper 90-2377 at the AIAA/SAE/ASME/ASEE 26th Joint Propulsion Conference, Orlando, FL, July 16-18, 1990; received Aug. 2, 1990; revision received April 15, 1991; accepted for publication April 15, 1991.

*Senior Group Engineer, Bldg. 4666, NASA Marshall Space Flight Center. Member AIAA.
†Senior Engineer, EP53. Member AIAA.

Introduction

THIS section presents an overview of the no-vent fill process, discusses the major problems associated with its modeling, and summarizes the objectives of this paper. It is followed by a more detailed description of the model's analytical structure, including the equations used to calculate transient thermodynamic behavior in different regions of the tank. The paper concludes by comparing code predictions with data from ground tests with Freon-114.

Description of No-Vent Fill Process

During a typical tank-to-tank transfer, pressure in the receiver vessel tends to increase due to ullage compression and mass transfer (i.e., boiling). In ground fill applications, this rise is compensated for by venting gas into the external environment. In a no-vent fill process, the pressure continues to rise until the receiver and supply tank pressures approach equilibrium. The only way to continue transfer is to reduce ullage mass by enhancing condensation across the gas/liquid interface. This is accomplished by either mixing the bulk fluid or agitating the liquid surface.

The process is essentially governed by two phenomena. Early on, when tank pressure differences are large, ullage compression limits the rate at which liquid enters the tank. Once the pressures approach equilibrium, however, the rate of ullage collapse caused by condensation regulates mass flow into the tank.

Problem

Developing computational models that accurately predict tank pressure histories and fill times demands a thorough accounting of the complex fluid mechanics, thermodynamics, and heat transfer occurring throughout the liquid, ullage, tank wall, and insulation. Most important, it requires a means of characterizing mass transfer, primarily in the form of condensation, across the liquid/ullage interface.

Precise modeling of mass transfer has been limited by three factors. First is the general lack of understanding regarding the chief mechanisms responsible for condensation and eva-

poration. This topic has received considerable attention,[1,2] primarily in correlating condensation mass flux with eddy effects and turbulence at the liquid surface.

The other two factors are due to inherent features of the spacecraft and its environment. Most obvious is the influence of microgravity, which promotes an indeterminate surface area at the gas/liquid interface. Typically, lack of acceleration forces will result in a larger exposed liquid surface for condensation. Modeling this variation will require an understanding of how fluid motion is affected by the tank's geometry and inlet flow regime.

The third factor involves the unique thermodynamic characteristics of cryogenic liquids. Because of their low boiling points and high thermal conductivities, the mass of propellant undergoing phase change is extremely sensitive to tank heating and mixing. Accurate predictions of pressure history and variations in other state properties will require a thorough account of heat flow into the propellant, mixing effects, and thermodynamic interactions between different regions in the fluid and tank volume.

The latter two factors, microgravity and cryogen thermodynamic behavior, are closely linked and must be considered simultaneously in any on-orbit fill model. However, the data needed to develop and validate empirical relationships for these effects are extremely limited. Only small-to-moderate-scale ground tests with simulated cryogens (e.g., Freon) and actual cryogens (e.g., hydrogen and nitrogen)[3] have been performed.

Until large-scale ground tests and small-to-medium-scale flight experiments[4] are conducted, computational development will focus on refining existing models within the context of current and prior ground tests. Once the condensation and thermodynamic relations in these models have been validated for a 1-*g* environment, theoretical models of microgravity effects will be incorporated and verified using results from planned flight tests.

Objective

The objectives of this paper are threefold. The primary purpose is to describe the field equations, constitutive relationships, and overall analytical structure of the FILL model.

The second objective is to show how the transient predictions of key state properties compare with results from no-vent fill tests using Freon-114. Pressurization histories for various fill rates and tank conditions were obtained using the Freon Test Article (FTA), a test bed designed for study of different inlet flow regimes. Test results from several bottom fill experiments have correlated well with the pressure behavior predicted by the model and have validated the program's use for future ground tests.

The third objective is to demonstrate the model's utility in evaluating current theories of condensation behavior. This effect is virtually impossible to measure and must be calculated from experimentally recorded state properties. This entailed running the FILL model in reverse to calculate condensation rates directly from test data. These rates were subsequently compared with predictions from universal submerged jet theory. Although the inlet jet arrangements on FTA tanks differ from those used in previous studies, the results show good agreement over the range of fill conditions encountered with the tests.

Model Description

The FILL model employs a finite difference analysis scheme that segregates the tank/fluid system into seven distinct control volumes or nodes. These include the ullage, bulk liquid, liquid/ullage interface layer, tank wall in contact with ullage, tank wall in contact with bulk liquid, and insulation surrounding each tank wall section.

The mass and energy flows between these regions are represented by a nodal network based on the transport quantities shown in Fig. 1. The nodal network provides a framework for

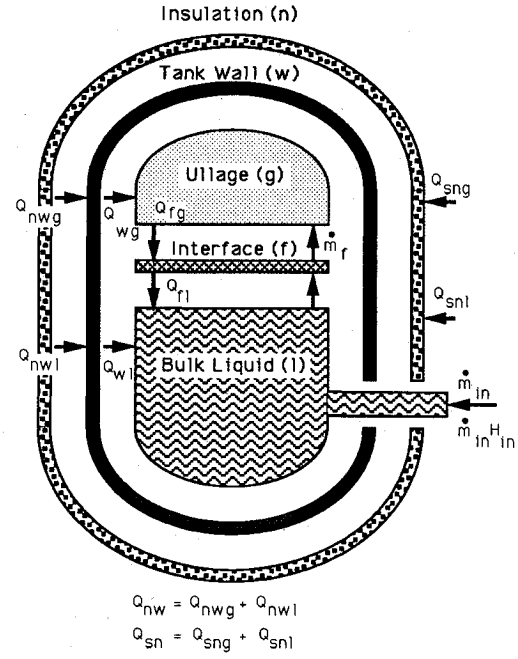

Fig. 1 FILL node and transport model.

representing these flows in terms of finite difference equations that are solved at each time step d*t*. Solution of the thermodynamic state variables, such as pressure and temperature, relies on a Taylor series expansion that truncates terms greater than first order and several constitutive relations that account for key physical processes.

One noteworthy aspect of the FILL model is the evaluation of surface condensation. The approach for representing this transport mechanism is based on the work of Hemlick et al.[1] and Brown et al.,[2] which considers condensation rate to be a function of bulk fluid properties and the liquid turbulence induced by jet geometry and orientation.

Mass Balance

During no-vent fill, only the gas and liquid regions in the tank undergo variations in mass. As shown in Fig. 1, liquid flow into the tank results in a corresponding mass addition to the bulk liquid. The only other form of mass transfer relevant to the process is condensation or boiling/evaporation across the liquid surface. The form that actually occurs depends on the relationship between thermodynamic states of the ullage and interfacial nodes. With these assumptions, the rate of mass change for the ullage is

$$dM_g/dt = m_f \tag{1}$$

The interface layer is assumed to be of infinitesimal thickness, and its mass is considered invariant. For the liquid node, the rate of mass change must account for the interfacial transfer as well as the mass introduced into the tank:

$$dM_l/dt = m_{in} - m_f \tag{2}$$

Energy Balance

The energy balance, which is also summarized in Fig. 1, is more complex and accounts for several modes of heat transport through the fluid, tank, and insulation. In the ullage, four transfer mechanisms are important: convection with the tank wall, convection with the liquid interface, compression work, and energy transported by interfacial mass transfer. Assuming the ullage to be a perfect gas yields the following energy balance:

$$M_g C_v dT_g/dt = Q_{fg} + Q_{wg} + w_g - m_f(H_{fg} - U_g) \tag{3}$$

For the interfacial region, compression work is ignored, thus leaving energy transferred via convection and mass transfer

$$Q_{fl} + Q_{fg} + m_f H_{fg} = 0 \tag{4}$$

For the bulk liquid, the energy balance must also consider the energy transported by fluid entering the tank. Because most liquids can be assumed incompressible, the work term is neglected, thus yielding the following equation:

$$M_l C_l \mathrm{d}T_l/\mathrm{d}t = Q_{wl} + Q_{fl} + m_f H_{fg} + m_{\mathrm{in}}(H_{\mathrm{in}} - H_l) \tag{5}$$

Energy balances through the tank wall and insulation are derived by applying a lumped mass approach, which assumes these nodes to be at uniform temperature. This yields the following energy balance for the tank wall adjacent to the liquid:

$$M_w C_w \, \mathrm{d}T_w/\mathrm{d}t = Q_{wl} - Q_{nw} \tag{6}$$

An expression similar to Eq. (6) is used for the section of tank exposed to the ullage.

FILL is capable of modeling two types of insulation in the outer node's energy balance: solid insulation (e.g., a foam-type material in which the primary mode of heat transfer is conduction) and radiation shields (e.g., aluminized mylar multilayer insulation, MLI, in which radiation is the principal mode). In addition, boundary conditions for the energy balance can be expressed in terms of either a fixed surface temperature or a specified heat flux. These options enable the modeling of many different storage scenarios and environments. Following is the balance for a foam-type insulation material with fixed boundary temperature (i.e., the equation used to compare FILL predictions with FTA tests):

$$M_n C_n \mathrm{d}T_n/\mathrm{d}t = Q_{nw} - Q_{sn} \tag{7}$$

Applying Eqs. (1-7) to the seven nodes shown in Fig. 1 provides the framework for deriving new values of tank pressure, fluid mass, temperature, and volume at each time increment. The next step is to define constitutive relationships that effectively reduce the problem to seven equations and seven unknowns. This involves expressing compressive work, heat transfer coefficients, and interfacial mass transfer in terms of known state variables. It also requires appropriate equations of state for the gas and liquid.

Constitutive Relationships

Compression work w_g appears in the energy balance for the ullage. For small time steps, this can be expressed by

$$w_g = P_g \mathrm{d}V_g/\mathrm{d}t \tag{8}$$

This term is iteratively evaluated based on a prior estimate of tank pressure at time $t + \mathrm{d}t$. Consequently, an approximate value is assumed for the first iteration pass. The iteration continues until the change in successive pressure estimates is less than a specified tolerance.

The rate of change of the gas volume is determined from the change in volume of the liquid and the slight change in total tank volume due to pressure:

$$\mathrm{d}V_g/\mathrm{d}t = -\mathrm{d}V_l/\mathrm{d}t + \mathrm{d}V_t/\mathrm{d}P_g \mathrm{d}P_g/\mathrm{d}t \tag{9}$$

For thick-walled tanks, the second term can be neglected. However, for thin-walled tanks, it is necessary to include this volume change.

Heat transfer rates between either fluid (i.e., ullage or liquid) and the tank wall are expressed in terms of Newton's law of cooling. The heat transfer coefficient h depends on the type of convection and flow conditions at the fluid/tank surface. For heat flux between the ullage and tank, free convection is assumed using the following general expression for h[5]:

$$h = (L/k)C(GrPr^n) \tag{10}$$

The coefficients C and n are constants that depend on whether the flow is laminar or turbulent ($GrPr > 10^9$ for turbulent). Free convection and equations similar to Eq. (10) are also assumed to estimate heat exchange across the tank/liquid and liquid/gas interfaces.

For calculation of total heat flow, the area of the wall/fluid interfaces are interpolated from tabular data that express exposed surface area as a function of tank volume. In addition, the interfacial area is assumed quiescent and is calculated from the tank diameter at the liquid/gas interface.

The form of interfacial mass transfer is determined by the fluid conditions at the given time step. An equation for liquid boiling is used when tank pressure falls below the liquid saturation pressure. Although this condition occurs for only a small portion of the initial fill, its effect is accounted for with the following expression[5]:

$$m_f = (P_{\mathrm{sat}} - P_t)/[\mathrm{d}P/\mathrm{d}m + \mathrm{d}P/\mathrm{d}t \times (H_{fg} - U_g)/m_g C_v] \tag{11}$$

Condensation is assumed whenever tank pressure exceeds the saturation pressure corresponding to the ullage temperature. Calculation of condensation rate utilizes an expression similar to the type developed by Brown et al.[2] It is derived by equating the equation for Stanton number St from universal submerged jet theory, namely,

$$St = m_{\mathrm{con}} H_{fg} Dd/[C_l (T_l - T_g) m_{\mathrm{in}} A_{\mathrm{con}}] \tag{12}$$

with an empirical relationship derived from previous studies,[1,2] namely,

$$StPr^{0.33} = 0.062 - 0.017 z/D \tag{13}$$

Note that this relation is restricted to applications in which $z/D < 3.0$.

When appropriate, ullage pressure, temperature, and volume are related using the perfect gas equation of state. Other thermophysical properties for the liquid and gas are evaluated with subroutines developed by the National Bureau of Standards.[6] These are based on the assumption of the fluid being a simple substance and essentially consist of functional relationships that express key properties, such as enthalpy, internal energy, thermal conductivity, specific heats, and density, in terms of at least two other state variables.

Model Validation

Test results from the FTA were used to evaluate the FILL model's predictive accuracy, check its theoretical and empirical constitutive relationships, and generally validate its use for ground fill analysis. The test article, a schematic of which is shown in Fig. 2, consists of three insulated tanks. During a typical no-vent fill, Freon-114 is transferred from the transfer tank to the 6.7-ft^3 receiver vessel, which has a mass/volume ratio of 5.0 and a maximum z/D of approximately 2.0.

The first step of the validation process compared the transient predictions of receiver tank state variables from FILL with FTA test data. This was useful not only for verifying the model's accuracy but also for assessing the no-vent fill process' sensitivity to key parameters, namely, fluid inlet temperature, liquid inflow rate, wall temperature, and condensation rate. Figure 3 shows a plot of receiver tank pressure from an FTA test in which the average flow rate and fluid inlet temperature were held at 39.5 gpm and 516°R, respectively. Initially, the tank pressure is lower than the fluid's saturation pressure. This causes boiling and a sharp pressure rise as liquid first en-

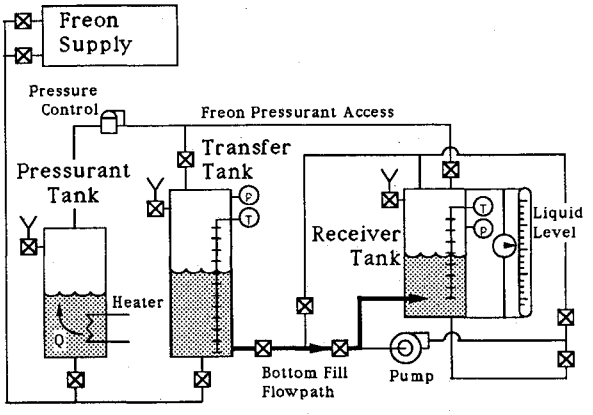

Fig. 2 Freon Test Article schematic.

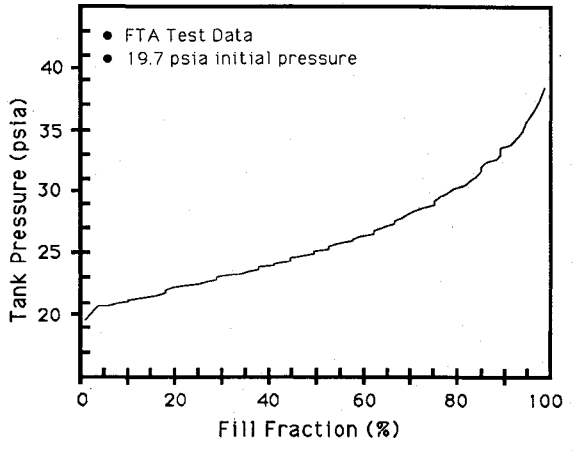

Fig. 3 Receiver tank pressure vs fill fraction.

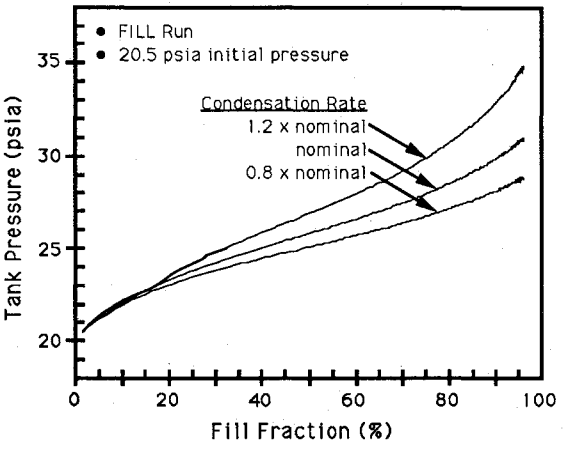

Fig. 4 Pressure sensitivity to surface condensation rate.

ters the tank. Boiling continues for only a few seconds until the tank pressurizes to a value greater than the liquid's saturation pressure. After this, the pressure rises slowly until the tank is approximately 80% full and then begins to increase at a higher rate. Probable causes for this sharp increase are the reduction in interfacial area as liquid fills the tank's top-dome section and the decrease in the condensation rate resulting from higher z/D.

The control of FTA test conditions was somewhat limited due to its outdoor location and exposure to the environment. This made a strict comparison between FILL and FTA results rather difficult. To accommodate the uncertainty in test conditions, FILL pressure transients were generated in a parametric form over a range of key parameter values. Liquid inflow rate and condensation rate were varied 20% from their nominal values. Liquid inlet temperature was varied by 4°R

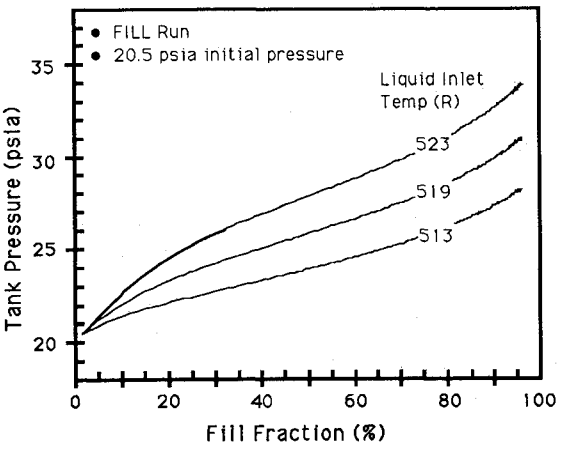

Fig. 5 Pressure sensitivity to liquid inlet temperature.

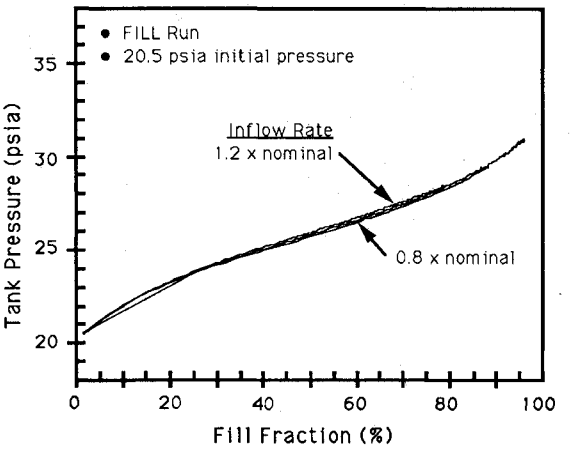

Fig. 6 Pressure sensitivity to liquid inflow rate.

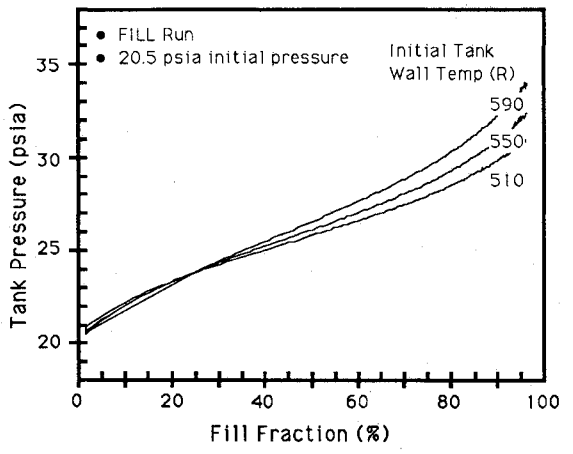

Fig. 7 Pressure sensitivity to initial wall temperature.

about a mean value of 519°R, whereas the initial tank temperature was varied by 40°R about a mean value of 550°R. Plots illustrating the sensitivity of pressure vs fill level (expressed as a percentage of the tank's volume) to these variations are shown in Figs. 4–7.

The notable differences in pressure transients in Figs. 4 and 5 indicate that condensation rate and liquid inlet temperature have the greatest influence on tank pressure. Surprisingly, the effect of inflow rate, as shown in Fig. 6, is relatively minor. This can be explained by the nature of the constitutive relationship in Eq. (12), which expresses condensation rate as linearly proportional to liquid inflow rate. Consequently, compressive effects, which are expected to increase with

higher flow rates, are offset by a corresponding increase in condensation.

The effect of wall temperature on ullage pressure is shown in Fig. 7. The relationship between the different traces indicates that wall temperature, at least for the FTA tests, does not play a critical role during the initial fill period. However, once the tank becomes approximately 50% full, wall temperature begins to play an important role.

A comparison between test data (Fig. 3) and model predictions (Figs. 4–7) indicates that the measured pressure fell within the range of test uncertainty. To better understand the difference between model and experiment behavior, the remaining validation focused on examining condensation rates derived from test data. This was done by reversing the FILL program logic and iteratively solving for condensation rate at each time step, thereby evaluating the functional relationship for z/D in Eq. (13). The iteration was driven by the convergence goal of matching the calculated pressure to within 0.05 psi of the measured value at each time step.

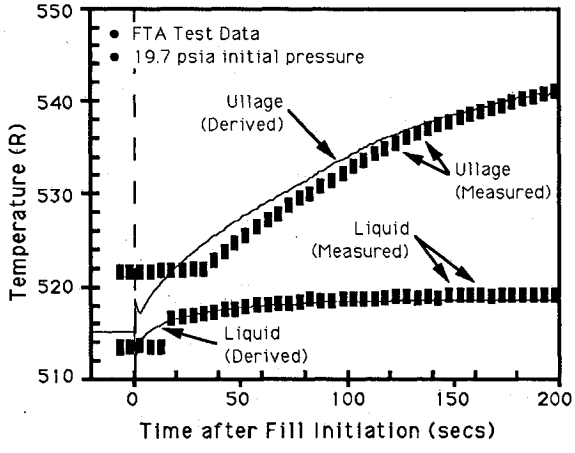

Fig. 8 Tank fluid temperature vs time.

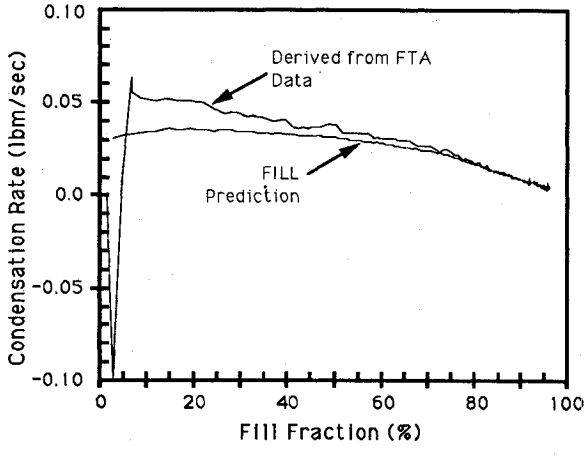

Fig. 9 Predicted vs derived condensation rate.

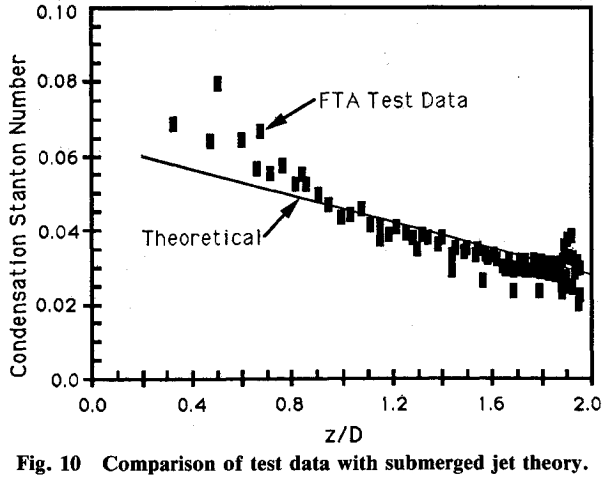

Fig. 10 Comparison of test data with submerged jet theory.

This approach also provided another means of evaluating FILL mass and energy relationships: it compared derived gas and liquid temperatures with measured values. Figure 8 shows such a comparison between calculated and measured values of gas and liquid temperature. The plot portrays the results from an FTA test in which the average flow rate and inlet temperature were held at 13.0 gpm and 518°R, respectively. A comparison between the actual and predicted trace indicates a very good correlation throughout the entire fill process and further substantiates the FILL program's mass and energy relationships.

Figure 9 shows a similar comparison between theoretical and derived condensation rates as a function of tank fill level. Except for a discrepancy early in the process, both traces exhibit reasonable correlation. The early discrepancy can be attributed to sudden evaporation as liquid initially enters the tank. FILL's boiling algorithm is somewhat limited in this regard because it requires the presence of a finite liquid volume in the tank prior to the transfer. Since this liquid is saturated at the tank's pressure, the bulk liquid temperature never increases sufficiently to cause boiling. However, as noted previously, this phase is brief in duration and the error in neglecting that effect is small.

A more general approach is to express the comparison in terms of nondimensional parameters. This is done by representing condensation rate in terms of Stanton number and by expressing time-dependent fill levels as discrete values of z/D. The relationship between Stanton number and z/D is shown in Fig. 10, which compares experimentally derived values obtained from several FTA bottom-fill tests with theoretical values calculated from Eq. (13).

At low z/D, the actual rate is slightly higher than theoretical predictions. In this range, the tank is only partially filled and susceptible to breakup of the liquid surface. This results in an increase in the exposed surface area and higher-than-predicted condensation rates. Thomas[7] observed similar behavior in an experiment that examined low values of z/D for axial jets.

This effect is compounded by the horizontal jet orientation in the FTA receiver tank, which enhances breakup during the initial phases of the fill process. Jet orientation is one of the major factors accounting for differences between derived values of condensation rate and predictions from the universal submerged jet model, which are based on an axial jet orientation. This is also evident when examining flow regimes in which $z/D > 1.0$. In this range, the derived condensation rates are slightly less than theoretical values. The horizontal jet orientation results in reduced surface turbulence and lower levels of condensation.

Conclusions

Comparisons of FILL analytical predictions with test results have confirmed the model's ability to evaluate no-vent fill in a 1-g environment. The paper has shown that the model's predictions of state properties correlate well with data from Freon-114 ground tests. It is expected that future no-vent fill tests with cryogenic fluids (e.g., hydrogen and nitrogen) will fully validate its use for 1-g applications. Eventually, when the data from flight tests become available, an advanced version of the code will be developed to account for microgravity effects.

In addition to transient predictions of tank thermodynamics, the model has also demonstrated its utility in supporting evaluations of condensation behavior. It was used to express data from a transient no-vent fill test in a form that enabled comparisons with tests run at static fill conditions. This procedure has further validated experimentally derived correlations with a moderately sophisticated system-level test. In fact, the ex-

cellent agreement between FTA results and theoretical predictions tend to support the universal submerged jet theory as a good approximation for nonaxial jets with $z/D < 2$.

Acknowledgments

The authors extend their appreciation to NASA Marshall Space Flight Center for use of ground test facilities and the Freon Test Article (FTA). The authors also wish to thank the following individuals for their significant contributions: W. Gilmore and R. Duane for conceiving and initiating design of the FTA, J. Cramer for originally organizing the FTA test program, and R. Carrigan and J. Hahs for operating the facility and conducting FTA tests.

References

[1]Hemlick, M., Khoo, B., Brown, J., and Sonin, A., "Vapor Condensation Rate at a Turbulent Liquid Interface, for Application to Cryogenic Hydrogen," AIAA Paper 88-0559, Jan. 1988.

[2]Brown, J., Hemlick, M., and Sonin, A., "Vapor Condensation at a Turbulent Liquid Surface in Systems with Possible Space-Based Applications," AIAA Paper 89-2846, July 1989.

[3]Moran, M., Nyland, T., and Papell, S., "Liquid Transfer Cryogenic Test Facility—Initial Hydrogen and Nitrogen No-Vent Fill Data," NASA TM-102572, March 1990.

[4]Jones, O., Meserole, J., Hedges, D., and Schmidt, G., "Conceptual Design of the Subscale Orbital Fluid Transfer Experiment (SOFTE)," AIAA Paper 90-2378, July 1990.

[5]Kreith, F., *Principles of Heat Transfer*, 3rd ed., Harper & Row, New York, 1976.

[6]McCarty, R., and Weber, L., National Bureau of Standards, TN-384, TN-617, and TN-648, July 1971.

[7]Thomas, R., "Condensation of Steam on Water in Turbulent Motion," *International Journal of Multiphase Flow*, Vol. 5.1, 1979, pp. 1-15.

James A. Martin
Associate Editor